ENERGY DISSIPATION OVER LARGE-SCALE ROUGHNESS FOR BOTH TRANSITION AND UNIFORM FLOW CONDITIONS

by [1]Stefano Pagliara, [2]Thendiyath Roshni, [2]Michele Palermo

Abstract: Rock chutes are natural river training structures and are efficient energy dissipaters too. From the hydraulic and environmental point of view, rock chutes have become important structures in the natural river morphology. A physical study was conducted and flow properties were measured over rough bed materials of a rock chute, which was assembled at the PITLAB center of the University of Pisa, Italy. Experiments were performed for slopes varying between $0.18 \leq S \leq 0.38$, $0.03 < d_c/H < 0.54$ and for ramp lengths L_r between 1.17 m $\leq L_r \leq$ 3.6 m. This paper presents the energy dissipation characteristics of the two-phase flows in the presence of two different base materials. In addition, the dissipative process was also analyzed in the presence of reinforcing boulders located on the base material. The findings showed that energy dissipation rate slightly increases with the boulder concentrations for the tested slopes and materials. The experiments were conducted for different rock chute lengths in order to understand its effect on the energy dissipation. An empirical expression is developed for determining the energy dissipation characteristics over different base materials in different ramp length conditions in two-phase flows. Results have been compared with the results obtained for stepped chutes and found a similar decreasing trend of dissipation rate for $d_c/L_r \leq 0.1$.

Keywords: energy dissipation, rock chute, boulders, two-phase flows

[1] Corresponding Author, Prof., DESTEC-Department of Energy Engineering, Systems, Land and Construction, University of Pisa, Via Gabba 22, 56122, Pisa, Italy, E-mail: s.pagliara@ing.unipi.it.

[2] Ph.D., DESTEC-Department of Energy Engineering, Systems, Land and Construction, University of Pisa, Via Gabba 22, 56122, Pisa Italy.

1. INTRODUCTION

Rock chutes are considered as one of the most effective energy dissipater. They are efficient river restoration structure, and plays a major role in river water quality improvement with particular attention to the natural river morphology dynamics. Recently, it has received a great attention because of its flexibility and capacity to conjugate hydraulic functioning and environmental care [1, 2, 3, 4, 5, 6]. The flow accelerates along the chute resulting in a two-phase flow in steep slopes and macroroughness conditions. However, the performance of rock chute structures in two-phase flow conditions is not well known in literature. In steep slopes and macro-roughness conditions [7], a strong interaction between the free surface and the bed material can occur, resulting in a two-phase flow towards the downstream part of the chute. Limited experimental researches in the past were conducted [8, 9, 10], in which the dissipative process over block ramps was analyzed without taking air presence in to account. In case of stepped spillways, several authors [11, 12, 13, 14] investigated the energy loss characteristics in two-phase flow conditions.

The present paper aims to analyze the energy dissipation process occurring in a narrow channel over large-scale roughness conditions for both transition and uniform flow conditions. The analysis was conducted varying the base material and with different reinforcing boulder arrangements. Boulders were located on the chute bed in different concentrations.

2. EXPERIMENTAL FACILITIES AND MEASUREMENTS

The experimental channel was 4 m long, 0.4 m high and 0.31 m wide, assembled at the PITLAB hydraulic laboratory of University of Pisa, Italy. The channel can be tilted to obtain the desired slope. At the end of the sloping chute, a horizontal channel of 2 m long and 0.31 m wide is provided. Experimental sloping channel is divided in to two flumes of width B =0.15m by a perspex wall 0.01 m thick each. Both the sloping channel and the downstream horizontal channel were narrowed using a perspex wall 0.01 m thick, resulting in a test channel whose width was 0.15 m. A pump allowed for discharge regulation up to Q=0.03 m^3/s, measured by means of a KROHNE OPTIFLUX 2000 KC electromagnetic flow meter of precision of 0.5%. Water is discharged in to the channel by means of an ogee crest in order to have a correct boundary layer development [15]. The rock chute has been prepared by gluing one layer of crushed stones downstream of the ogee crest. Experiments were

conducted using two base materials: material M_{R1}, whose granulometric characteristics are D_{16} = 38.17 mm, D_{50} = 43.41 mm and D_{84} = 47.17 mm and material M_{R2}, whose granulometric characteristics are D_{16} = 105.8 mm, D_{50} = 120 mm and D_{84} = 149 mm. D_{xx} is the diameter for which xx% in weight of material is finer. For material M_{R1}, x_o/D_{84}=8.8 and for material M_{R2} x_o/D_{84}=8.93, where x_o is the ogee curvilinear crest length (see fig. 1a-b). Considering an average prototype block ramp material diameter D_{50} ranging between 0.60 m and 0.80 m, models scales lie between λ_{R1}=1:15 and λ_{R2}=1:5 respectively, where λ is the length scale ratio. For the tested conditions and discharges, the aspect ratio of flumes falls into the narrow channel condition (d/B<5) [16] where d is the flow depth. The flow in large scale roughness condition is strongly three dimensional [17] and the flow mixing and secondary flows due to the interaction with the base material generally overcomes the turbulence due to the secondary flows by side walls and hence the side wall effect can be neglected. The air concentration along the chute was recorded using an USBR air concentration meter (ACM) with the help of an intrusive single tip conductivity probe of tip Ø6 mm [18], which was aligned along the flow direction. The air concentration probe was fixed to a point gauge 0.1 mm precise in order to measure the air concentration at different depths vertically. The probe was carefully calibrated before the tests beginning and each measurement was sampled for 30-40s with a sampling rate of 15 kHz. For each selected transversal section, measurements were taken in several points belonging to vertical sections located at $z=B/4$, $B/2$ and $3B/4$ (see fig. 1c). The air concentration measurements were averaged at three transversal sections towards the end of the rock chute, where the flow achieves nearly uniform flow condition over the material M_{R1} [18]. The average air concentration C_m in each vertical section is calculated as

$$C_m = (1/y_{90}) \int_{y=0}^{y=y_{90}} C dy \quad (1)$$

where, y_{90} is the depth normal to the bed for C=90% and C_m is the average air concentration for each transversal section.

Figure 1 shows the diagram sketch of the experimental apparatus and the aerated flows over M_{R1} and M_{R2} base materials. h_0 is the flow depth at section 0-0 (ogee crest end) and h_1 is the flow depth at the horizontal basin at section 1-1, H is the ramp height at entrance. Section 1-1 is located at a distance L_d

from the chute varying between 60 cm and 90 cm, in which the water flow was practically deaerated. S=tanα is the channel slope, P.T is the physical top of the blocks in base configuration, E.T is the effective top, which is $0.2D_{65}$ lesser than P.T. x is the longitudinal coordinate from the ogee crest end and y is the normal coordinate of the rock chute measured from the P.T [18]. E_0 is the total upstream energy at section 0-0, whereas E_1 is the energy at the toe of the rock chute ($E_1=h_1+(V^2/2g)$). Hence, the relative energy loss is $\Delta E_r=\Delta E/E_0$, where $\Delta E=E_0- E_1$ and V is the average flow velocity at the section 1-1. Experiments were also performed by placing boulders (in row and staggered arrangements) whose mean diameter is D_B=55 mm at different boulder concentration $\Gamma=N_B\pi D_B^2/(4BL_r)$=0, 0.05, 0.15, and arrangement (rows and random), where N_B is number of boulders.

Fig. 2 shows the flow characteristics over base materials M_{R1} (S=0.38) and M_{R2} (S=0.18), where d_e is the effective water depth ($d_e = 0.2D_{65} + \int_{y=0}^{y=y_{90}} (1-C)\, dy$), d_c is the critical depth and x is the longitudinal co-ordinate, according to the reference system shown in fig. 1a-b. For base material M_{R1}, the flow characteristics show that the flow nearly reaches uniform flow condition towards the channel end, but in M_{R2}, due to its limited length, the flow is still in transition region [17]. The flow depth and the bed profile were measured using a point gauge with a precision of 0.1 mm. Experiments were conducted for slopes S ranging between $0.18\leq S\leq 0.38$ and for ramp lengths L_r between 2.0 m $\leq L_r\leq$3.6 m for base material M_{R1} and 1.17 m $\leq L_r\leq$2.74 m for base material M_{R2}. Fig. 3 shows the aerated flows over base materials M_{R1} and M_{R2} at S=0.38, where q is the discharge per unit width.

The characteristics of the tested flows are shown in Table 1. The data of the experimental runs which lies in the large-scale roughness [7] are selected for the present study. In Table 1, C_u is the mean of C_m in uniform flow region [18].

3. EXPERIMENTAL RESULTS AND DISCUSSION

3.1 Energy dissipation and aeration

In the tested range of parameters, mostly large-scale roughness conditions occurred [7]. The dissipative process was analyzed along the base chute (*i.e* without boulders). Fig. 4a shows the rate of energy dissipation along the chute ($\Delta E_{r(x)}$) from the ogee crest end (section 0-0) to the toe of the rock chute. Here $\Delta E_{r(x)}$ is calculated based on equivalent depth d_e estimated in the transversal section whose distance from the section 0-0 is x (see fig. 1). $\Delta E_{r(x)}$ is calculated as E_o-E_x/E_o, where

$E_x = H_x + d_e \cos\theta + V_w^2 / 2g$ [19] is the residual head at the selected section, in which $V_w = Q/(B.d_e)$ and H_x is the ramp height at x distance.

Tested data are compared with those derived from [20] for smooth chute and stepped chute for a slope of 4 degrees. The energy dissipation trend over the rock chute is found similar to that of smooth and stepped chute. This is due to the occurrence of some similar flow characteristics over the rock chutes and the stepped chutes [18]. It is observed that rate of increase of energy dissipation is faster at the upstream part of the chute when compared to the aerated flow near to toe of the rock chute. Significant losses in the upstream part is due to the nappe flow impact and when air entrainment occurs, energy losses are mainly due to the high splashing and vortex shedding between the ramp elements. For each slope, greater energy dissipation is occurred at larger flow rates at the upstream end as also observed for stepped chutes by [20] . Fig. 4b denotes the residual head measured over the base materials M_{R1} and M_{R2}. Residual head were compared at same ramp length for different d_c/D_{84}. The comparison of residual energy between the two materials show that the average value of the residual energy for each slope is independent of the material size and discharge [21].

3.2 Effect of ramp length and boulders concentration on energy dissipation

For all flow configurations over M_{R1} and M_{R2} materials, a decreasing rate of energy dissipation is observed for increasing discharges as it was observed in previous studies over stepped spillways and block ramps [9, 19]. The effects of ramp length and different base materials on energy dissipation rate (ΔE_r), for the tested configurations with and without boulders and for two different tested slopes, are shown in figs. 5(a-b). In fact, keeping constant discharge, the differences between ΔE_r for the tested L_r in the same base configuration are negligible.

When compared to the base configuration, ΔE_r slightly increases with the boulder concentration for tested slopes and materials. The increase is more evident for boulders over base material M_{R1} (D_B/D_{84}=1.17), whereas practically it is almost negligible for base material M_{R2} (D_B/D_{84}=0.37). This is due to the fact that for base material M_{R1} the boulders are protruding more than for base material M_{R2}, thus generating a bigger flow disturbance. But just for design purposes, the effect of boulder concentrations and arrangements can be neglected in the tested range of parameters (Γ<0.15). Moreover, the difference in the dissipation rate for M_{R1} and M_{R2} base material are also negligible, as

the experiments were conducted for large-scale roughness conditions. Based on the experimental observation, an empirical expression was developed for estimating ΔE_r valid in the range of $0.18<S<0.38$, $d_c/L_r \leq 0.1$ and $\Gamma \leq 0.15$:

$$\Delta E_r = 0.33 + (1 - 0.33) \cdot e^{(30 \cdot S - 17.5) \cdot (d_c / L_r)} \quad (2)$$

Fig. 6a illustrates the dependence of ΔE_r on d_c/L_r for all slopes and tested conditions. Similar decreasing trend of dissipation rate for $d_c/L_r<0.1$ can be observed also for stepped chutes and is shown in fig. 6b, in which the data of [12, 22] are reported.

4. CONCLUSIONS

This paper analyzed the dissipative process occurring over rock chutes with two base materials M_{R1} and M_{R2} and for different boulders configurations in two-phase flow conditions. Different ramp lengths and boulder concentrations were tested. The analysis of data along the rock chute shows that the energy dissipation rate is larger at the upstream part of the chute compared to the downstream end. It was proved that, in the tested range of parameters, the effect of boulder arrangements and its concentration on the relative energy dissipation has negligible effects respect to the base configuration for practical purposes. An empirical equation was developed to predict the dissipation rate. The proposed relation is valid in the tested range of parameters. Further detailed research is needed in order to assess the role of the air concentration on the energy dissipation.

5. NOTATION

The following symbols are used in this paper:

B = channel width

C = void fraction (volume of air per unit volume); also called as air concentration

C_m = depth averaged air concentration defined in terms of y_{90}

C_u = average air concentration in the uniform flow region

D_B = mean diameter of boulders

d =flow depth

d_c = critical flow depth

D_{xx} = characteristic diameter of the bed material for which xx % of material is finer

$\Delta E_{r(x)}$ = energy dissipation rate along the chute

ΔE_r = relative energy dissipation

E_x = residual head at different longitudinal sections

E_o = total energy at section 0-0

E_1 = total energy at section 1-1

h_o = flow depth at section 0-0

h_1 = averaged flow depth at section 1-1

H = height of the ramp

H_x = ramp height along x co-ordinate

L_r = length of ramp

Ø = conductivity probe diameter

Q = water discharge

q = discharge per unit width

S = tanα; channel slope

N_B =no. of boulders

V = average flow velocity

L_d =Length from ramp toe in the chute to flow zone with no air

x = longitudinal distance along the channel bottom

x_o = ogee curvilinear crest length

y = vertical coordinate measured from the *P.T.*

y_{90} = depth in which the air concentration C equals 90%

Γ = boulder concentration

λ_l = model scale

6. LIST OF REFERENCES

[1] Pagliara S., Palermo M., Rock grade control structures and stepped gabion weirs: scour analysis and flow features, Acta Geophysica, 2013; 61 (1), 126-150.

[2] Pagliara S., Palermo M., Carnacina I., Live-bed scour downstream of block ramps for low densimetric Froude numbers, International Journal of Sediment Research, 2012; 27 (3), 337-350.

[3] Pagliara S., Palermo M., Effect of stilling basin geometry on clear water scour morphology downstream of a block ramp, Journal of Irrigation and Drainage Engineering, 2011; 137 (9), 593-601.

[4] Pagliara S., Palermo M., Block ramp failure mechanisms: critical discharge estimation, Proceedings of the Institution of civil Engineers-Water Management, 2011; 164 (6), 303-309.

[5] Pagliara S., Palermo M., Carnacina I., Expanding pools morphology in live-bed conditions, Acta Geophysica, 2011; 59 (2), 296-316.

[6] Pagliara S., Palermo M., Scour control and surface sediment distribution downstream of block ramps, Journal of Hydraulic Research, 2008; 46 (3), 334-343.

[7] Bathurst J.C., Flow resistance estimation in mountain rivers, Journal of Hydraulic Engineering, 1985; 111 (12), 625-643.

[8] Ahmad Z., Petappa N.M., Westrich B., Energy dissipation on block ramps with staggered boulders, Journal of Hydraulic Engineering, 2009; 135 (6), 522-526.

[9] Pagliara S., Chiavaccini P., Energy dissipation on block ramps, Journal of Hydraulic Engineering, 2006; 132 (1), 41-48.

[10] Pagliara S., Chiavaccini P., Energy dissipation on reinforced block ramps, Journal of Irrigation and Drainage Engineering, 2006; 132 (3), 293-297.

[11] Chanson H., Comparison of energy dissipation between nappe and skimming flow regimes on stepped chutes, Journal of Hydraulic Research, 1994; 32 (2), 213-219.

[12] Chanson H., Toombes L., Energy dissipation and air entrainment in stepped storm waterway: Experimental study, Journal of Irrigation and Drainage Engineering, 2002; 128 (5), 305-315.

[13] Christodoulou G.C., Energy dissipation on stepped spillways, Journal of Hydraulic Engineering, 1993; 119 (5), 644-650.

[14] Sorensen R.M., Stepped Spillway Hydraulic Model Investigation, Journal of Hydraulic Engineering, 1985; 111 (12), 1461-1472.

[15] Ohtsu I., Yasuda Y., Takahashi M., Discussion of `Characteristics of skimming flow over stepped spillways' by M.R. Chamani and N. Rajaratnam, Journal of Hydraulic Engineering, 2000; 126 (11), 869-870.

[16] Chow V.T., Open channel hydraulics, McGraw-Hill Book Co., New York. (1959).

[17] Pagliara S., Carnacina I., Roshni T., Inception point and air entrainment on flows under macro-roughness condition, Journal of Environmental Engineering, 2011; 137 (7), 629-638.

[18] Pagliara S., Carnacina I., Roshni T., Self-Aeration and Friction over Rock Chutes in Uniform Flow Conditions, Journal of Hydraulic Engineering, 2010; 136 (11), 959-964.

[19] Felder S., Chanson H., Energy dissipation down a stepped spillway with non-uniform step heights, Journal of Hydraulic Engineering, 2011; 137 (11), 1543-1548.

[20] Chanson H., Toombes L., Energy dissipation in stepped waterway, Energy and water: Sustainable development, ASCE, San Francisco, CA, 1997; 595-600.

[21] Felder S., Chanson H., Energy dissipation and residual energy on embankment dam stepped spillways, Water engineering for a sustainable environment - 33rd IAHR Biennial Congress, Vancouver BC, Canada, 2009; 1940-1947.

[22] Barani G.A., Rahnama M.B., Sohrabipoor N., Investigation of flow energy dissipation over different stepped spillways, American Journal of Applied Sciences, 2005; 2 (6), 1101-1105.

7. LIST OF TABLES

Table 1. Experimental tests characteristics

Bed material	x_o/D_{84}	S	q (m^2/s)	d_c/H	C_u	D_B/D_{84}
M_{R1}	8.8	0.18	0.017-0.17	0.07-0.34	0.14-0.19	1.17
		0.275	0.033-0.17	0.05-0.15	0.18-0.30	1.17
		0.38	0.017-0.17	0.04-0.17	0.26-0.50	1.17
M_{R2}	8.93	0.18	0.033-0.12	0.09-0.54	-	0.37
		0.275	0.017-0.10	0.04-0.14	-	0.37
		0.38	0.017-0.10	0.03-0.19	-	0.37

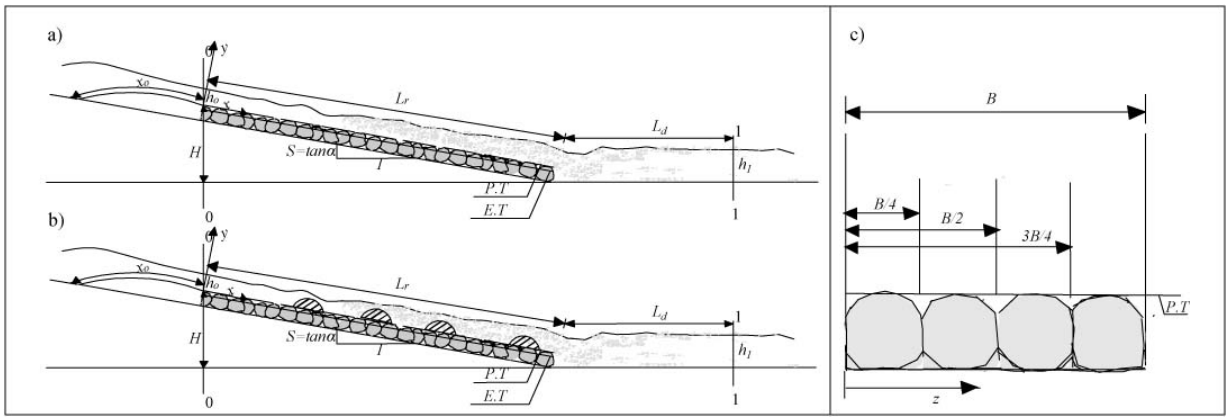

Fig. 1 Diagram sketch of the experimental apparatus with notations a) for base and b) reinforced configurations and c) Channel transversal section

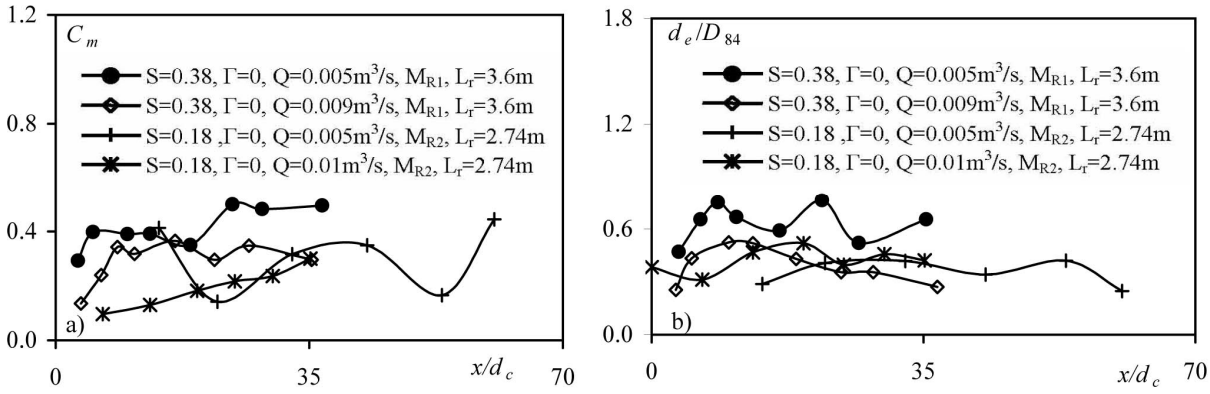

Fig. 2 Flow characteristics a) average concentration (C_m) and b) relative equivalent depth (d_e/D_{84}) over base material M_{R1} and M_{R2} at S =0.38 and S=0.18

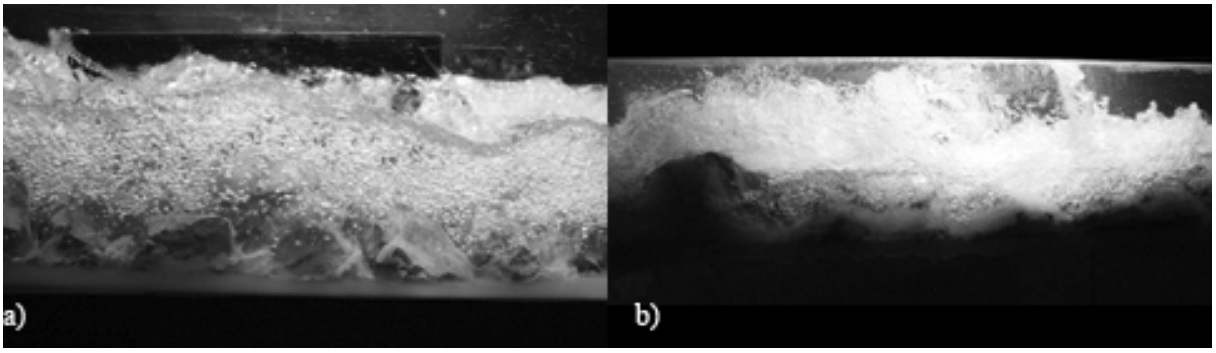

Fig. 3 Aerated flows over a) M_{R1} materials at S = 0.38, q = 0.03m^2/s and b) M_{R2} material at S = 0.38, q= 0.1 m^2/s (flow from the left).

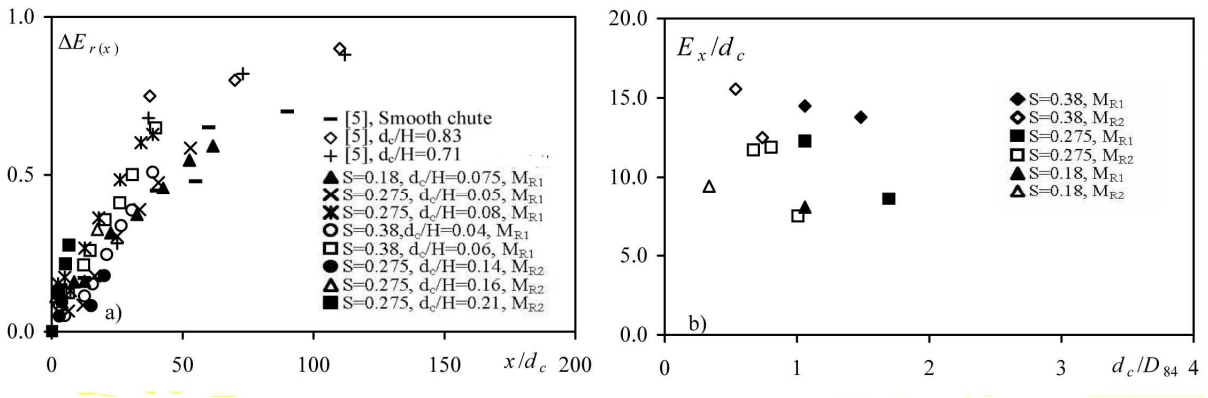

Fig. 4 a) Rate of energy dissipation over ramp length for base material configurations M_{R1} and M_{R2} and comparison with [20] data for S=0.07; (b) dimensionless residual energy at the end of the sloping channels.

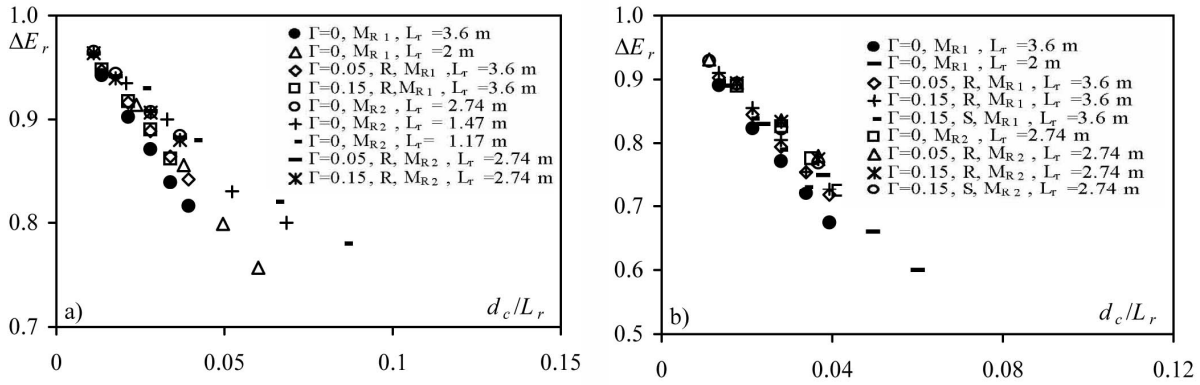

Fig. 5 Energy dissipation rate over different boulder concentrations in row (R) and staggered (S) manner over M_{R1} and M_{R2} channels a) for S=0.38 and b) S=0.18

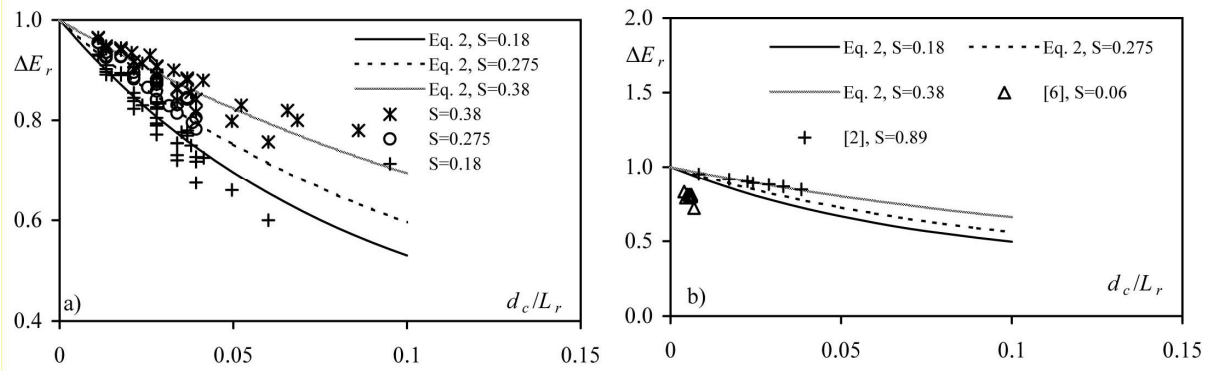

Fig. 6 a) Relation between the energy dissipation rate and d_c/L_r, (b) comparison between eq. (2) and other data derived from literatures for stepped chutes.

8. LIST OF FIGURES

Figure 1. Diagram sketch of the experimental apparatus with notations a) for base and b) reinforced configurations and c) Channel transversal section

Figure 2. Flow characteristics a) average concentration (C_m) and b) relative equivalent depth (d_e/D_{84}) over base material M_{R1} and M_{R2} at S =0.38 and S=0.18

Figure 3. Aerated flows over a) M_{R1} materials at S = 0.38, q = 0.03m^2/s and b) M_{R2} material at S = 0.38, q= 0.1 m^2/s (flow from the left).

Figure 4 a)Rate of energy dissipation over ramp length for base material configurations M_{R1} and M_{R2} and comparison with [20] data for S=0.07; (b) dimensionless residual energy at the end of the sloping channels.

Figure 5. Energy dissipation rate over different boulder concentration in row (R) and staggered (S) manner over M_{R1} and M_{R2} channels a) for S=0.38 and b) S=0.18.

Figure 6. Relation between the energy dissipation rate and d_c/L_r, (b) comparison between eq. (2) and other data derived from literatures for stepped chutes